

SUPPORTING MATERIALS AND METHODS

Materials

Human fibrinogen (free of plasminogen, von Willebrand factor and fibronectin) in 20 mM sodium citrate and human α -thrombin was purchased from Enzyme Research Laboratories (South Bend, IN). Factor XIII is present in the fibrinogen solution (1). Centrifuge filtration units with a 100 kDa molecular weight cut off were from Millipore Corp (Billerica, MA). Prostacyclin (PGI₂) was from Cayman Chemicals (Ann Arbor, MI). #88 T316 stainless steel mesh with 200 μ m openings was from TWP Inc. (Berkeley, CA). 10% (by weight) sodium dodecyl sulphate (SDS) solution, 40% Acrylamide (19:1 Acrylamide:Bis-acrylamide) solution, Ammonium persulphate (APS), tetramethylethylenediamine (TEMED), 2-mercaptoethanol (β ME), 10x premixed electrophoresis buffer (containing 25 mM Tris, 192 mM glycine, pH 8.3), 4x Laemmli protein sample (containing 277.8 mM Tris-HCl, pH 6.8, 4.4% LDS, 44.4% (w/v) glycerol, 0.02% bromophenol blue), Tris base, Precision Plus Protein™ Kaleidoscope™ Standards (10-250 kDa) and Bio-safe Coomassie Blue stain were all purchased from Bio-Rad (Hercules, CA). Tris buffer was prepared by dissolving 1.5 M Tris base in deionized water and pH 8.8. All other chemicals were purchased from Sigma-Aldrich (St. Louis, MO). Tris buffered saline (TBS; 50 mM tris base, 100 mM NaCl, pH 7.4), modified Tyrode's buffer (129 mM NaCl, 20 mM HEPES, 12 mM NaHCO₃, 2.9 mM KCl, 1 mM MgCl₂, 0.34 mM Na₂HPO₄ · 12H₂O, pH 7.3), acid-citrate dextrose (ACD; 0.085 M sodium citrate 0.085 M, 0.11 M D-glucose, 0.071 M citric acid monohydrate), and sodium citrate solutions (0.13 M, pH 9.1) were made in house. AlexaFluor 555 labeling kit was purchased from Life Technologies (Grand Island, NY).

Preparation of fibrin gels

Fibrinogen stock solutions were prepared as previously described (38). Briefly, fibrinogen stock solutions (12.9 mg/mL) were centrifuged at 4000 g at 37 °C for 2 h in filtration units. After centrifugation the retentate was removed from the device and diluted in TBS. The concentration of fibrinogen in the retentate was determined by using a modified Clauss assay to measure the concentration of a known dilution of retentate to achieve a ~1 mg/mL fibrinogen solution (see Supporting Methods); 10 nM thrombin and 2.5 mM CaCl₂ were added to 100X diluted retentate in a 96 well plate (200 μ L final volume) (39, 40). After 20 min, the absorbance was measured in a plate reader (Victor X, PerkinElmer) and the concentration was determined from a standard curve. Both the concentrated fibrinogen stock solution and fibrinogen in sodium citrate were tested for the presence of aggregates by dynamic light scattering with a size range of 1 nm — 10 μ m (Zeta PALS, Brookhaven Instruments, Holtsville, NY). Fibrinogen solutions of 3, 10, 30, 50, and 100 mg/ml in TBS were mixed with 2.5 mM CaCl₂ (final concentration) and 10 or 100 nM thrombin (final concentration).

To determine the extent of conversion of fibrinogen to fibrin gels a test was conducted in which gels were allowed to form for 50 min after which excess buffer was added to the gels to capture any unincorporated fibrinogen for testing. Fibrin gels (0.5 mL) identical to those used for rheological testing were formed in 24-well plates for 50 min. After gelation, an additional 0.5 mL TBS was pipetted onto the top of each gel. The gel-TBS mixtures were homogenized with a glass rod and incubated for 24 h to allow any unincorporated fibrinogen to diffuse out of the formed gel and into the TBS. After incubation the visible particles of the broken clot were

Supporting Material

removed from the disrupted gel-TBS mixture by filtering the mixture through a screen with $200\ \mu\text{m} \times 200\ \mu\text{m}$ pores. The remaining filtrate was tested for the presence of unreacted fibrinogen by polymerizing any unreacted fibrinogen present in the filtrate; CaCl_2 (2.5 mM) and thrombin (10 nM) were added to the filtrate to induce gelation and the modified Clauss assay was used to determine the concentration of the fibrin in the gel.

Modified Clauss Assay

Ten milliliters of stock fibrinogen solution at 12.9 mg/ml were dialyzed against TBS and then reduced to ~ 1 mL by centrifuging the solution at 37°C in a centrifugal concentrator device with a molecular weight cutoff of 100,000 Da. The concentration of the resulting retentate solution is ~ 129 mg/mL fibrinogen. A sample of this concentrated solution is diluted to ~ 1 mg/mL in TBS and 10 nM thrombin and 2.5 mM CaCl_2 (final concentrations) are added to induce gelation. The absorbance of this gel is measured at 405 nm and compared to a standard curve (dynamic range 0-1.5 mg/mL) to determine a more accurate concentration of the diluted sample. The initial estimate for the retentate solution concentration (129 mg/mL) is then refined based on the measured concentration of the diluted sample (e.g. if the diluted sample was determined to have 1.05 mg/ml fibrin instead of 1.0 mg/ml fibrin the initial estimate would be scaled by 1.05/1 to give a value of 135 mg/ml).

To validate this method, we compared value the concentration of fibrinogen as determined by the modified Clauss assay to the concentration of a 400X diluted retentate sample as determined by absorbance at 280 nm using a UV/VIS spectrophotometer with an extinction coefficient of $1.51\ \text{ml}\ \text{mg}^{-1}\ \text{cm}^{-1}$ (2). The concentrations of the fibrinogen retentate as determined by the modified Clauss assay (129 ± 4 mg/ml) was found to be in good agreement with the value determined by UV/VIS (125 ± 2 mg/ml).

Solubility of fibrinogen solution

One hundred microliters of concentrated fibrinogen (~ 130 mg/ml) and fibrinogen stock solution (12.9 mg/ml) were pipetted into the wells of a clear, flat-bottomed 96-well plate. Solutions were incubated at 4, 20, and 37°C and the absorbance at 450 nm of was measured over a period of 45 hours to determine solubility (3). Each condition was done in triplicate. The absorbance of both the concentrated fibrinogen and the stock fibrinogen incubated at 4°C increased with time indicating precipitation of fibrinogen (Fig. S2). This precipitation was also observed by transition from a clear to cloudy solution. The absorbance of the same fibrinogen solutions incubated at 21°C and 37°C did not change of over the period of 45 hours indicating the fibrinogen remained in solution.

SDS-PAGE Analysis of Fibrin Cross-linking

Fibrin gels identical to those use in the mechanical testing experiments were formed with 3, 10, 30, 50, and 100 mg/ml fibrinogen and 10 nM thrombin (final concentrations) and allowed to gel for 50 minutes. Ligating reactions in the samples was quenched with 6 M urea, and 2% SDS at 37°C for 2 h. Gel electrophoresis (8% polyacrylamide) was prepared using standard protocols (4). Briefly, to make one gel, 1.6mL 40% acrylamide solution, 2 mL 1.5M Tris buffer, 80 μL

Supporting Material

each of 10% SDS solution and 10% (by weight) of APS solution and 8 μL of TEMED to 4.2mL of deionized water. The solution was mixed, cast into a mini gel 1 mm thick and allowed to polymerize for 45 minutes. Samples for electrophoresis were prepared by diluting proteins to $\sim 12 \mu\text{g}$ of total protein in deionized water and adding 4x Laemmli loading buffer (1:3 loading buffer:sample). Total volume of $\sim 25 \mu\text{L}$ of sample was loaded in each well. Proteins were fractionated into bands by electrophoresis running at 110 V for 90 minutes. Protein bands were visualized by staining with Coomassie blue stain for 1.5 h followed by washing in deionized water. The gels were then imaged on an Alpha Innotech IS2200 digital UV-Vis imaging system (Santa Clara, CA). Fig. S3 shows the results of the gel and demonstrates cross-linking for all fibrin gels.

Confocal microscopy of fibrin gels

Fibrin gels were prepared for confocal microscopy were prepared exactly as described above, except that samples were formed between glass slide and a #1 glass coverslip. Fibrinogen was labeled with AlexaFluor® 555 according to the manufacturer's instructions and was added to each solution at a molar ratio of 500:1 unlabeled:labeled fibrinogen. Images were captured on a laser scanning confocal microscope (Olympus Fluoview FV10i) using a 60X objective (NA = 1.2) and excitation/emission wavelengths of 556/573 nm.

SUPPORTING CALCULATIONS

Calculating the bending modulus of an individual fibrin filament

The persistence length of a bundle of fibers relative the persistence length of the sub-filaments within the bundle can be calculated using Eq. 2 from Bathe et al. (5):

$$\frac{\kappa_B}{\kappa_f} = N \left(1 + \frac{\chi^2 (N-1)}{1 + c(q_j) \frac{N + \sqrt{N}}{\alpha}} \right) \quad (\text{S1})$$

where, κ_B , is the bending modulus of the bundle, κ_f , is the bending modulus of the sub-filament, N , is the number of sub-filaments or protofibrils, α , is a fiber coupling parameter, c , is the wave number, and χ is a parameter accounting for the finite thickness of the crosslinks. For the fully decoupled (no cross-linking) case, $\alpha = 0$ causing the bracketed term to be equal to unity.

However, fibrin fibers are cross-linked by factor XIIIa in our rheology measurements (Fig. S3). The bending modulus of coupled (cross-linked) and decoupled (not cross-linked) fibrin filaments has been reported as 14.5 MPa and 1.7 MPa, respectively (6). Based on these values, we estimate the bending modulus of a fibrin filament to be 8.5 times greater (14.5/1.7) than the bending modulus of a bundle of fully uncoupled sub-filaments, reducing Eq. S1 to:

$$\kappa_B = 8.5N\kappa_f \quad (\text{S2})$$

For the protofibrils within our gels, N is calculated using Eq. 6 from Weigandt et al. (7),

$$N = \frac{\Phi_{\text{int}} \rho_m R^2}{\mu_p} \quad (\text{S3})$$

where Φ_{int} , is the internal volume fraction of the fibrin filament, and ρ_m and μ_p are the mass density and the mass to length ratio of a protofibril, equal to 1.4 mg/ml, and 340 kDa/22.5 nm, respectively (8). The value for R used is the previously measured hydrated fiber radius (9). The internal volume fraction, Φ_{int} , is a function of fibrinogen concentration and is based on a fit of the data presented in Fig. 5 in Weigandt et al.(7):

$$\Phi_{\text{int}} = 0.015 \ln(c_{fbg}) + 0.13 \quad (\text{S4})$$

Using the above values, $N = 30$ for the filaments within out network.

Finally, we are able to estimate the bending modulus of a fibrin filament based on the persistence length of a protofibril. The bending modulus of a protofibril is related to persistence length of a protofibril by:

$$\kappa_f = L_{p,f} k_B T \quad (\text{S5})$$

Supporting Material

where $L_{p,f}$ is the persistence length of a protofibril previously measured to be 500 nm (10). We can then estimate the bending modulus of a fibrin filament to be 4.5×10^{-24} Nm² by combining Eq. S2-S5 to obtain

$$\kappa_B = 8.5L_{p,f}Nk_B T \quad (\text{S6})$$

Estimating the nonaffine-affine transition of fibrin gels as a function of fibrinogen concentration

The nonaffine-affine (NA-A) transition length for fibrous networks can be predicted based on the filament length, L_c , mesh size, ξ , filament stretching modulus, μ , and filament bending modulus, κ_B (11). Affine deformations become more favorable when filament length becomes larger than a critical length, λ_{NA} , defined as:

$$\lambda_{NA} = \frac{\xi^2}{L_b} \quad (\text{S7})$$

and L_b is the characteristic bending length scale defined as a filament's susceptibility to bending verses stretching:

$$L_b = \sqrt{\frac{\kappa}{\mu}} \quad (\text{S8})$$

Therefore, if $L_c/\lambda_{NA} \gg 1$ an affine, stretching dominated regime is expected whereas if $L_c/\lambda_{NA} \ll 1$ a nonaffine, bending dominated regime is expected. The stretching modulus, μ , is estimated to be 5 nN by assuming the stretch modulus of a filament is equal to the sum of the stretch modulus of the protofibrils within the bundle. This value is consistent with a previous estimate of ~10 nN for fibers with slightly larger diameters (12). The stretch modulus of an individual protofibril is estimated to be 1.70×10^{-10} N with a corresponding length of 80 nm (13), assuming 30 protofibrils per bundle ($N = 30$), giving μ of 5×10^{-9} N. Using this value and the value for bending modulus calculated previously, the characteristic bending length, L_b , of a fibrin filament is calculated to be 30 nm. Combining L_b with estimates of mesh size as determined by permeability experiments allows us to calculate the NA-A transition length for each gel tested. Table S3 shows the calculated L_c/λ_{NA} for fibrin gels based on the methods describe above.

Estimating displacement of a fibrin caused by the platelet contractile force

The centerline bending displacement, δ_{bend} , caused by a force imparted on a simply supported beam is given by:

$$\delta_{bend} = \frac{F_{plt}\xi^3}{48\kappa_B} \quad (\text{S9})$$

Supporting Material

where F_{plt} is the maximum contractile force of a platelet, κ_B is the filament bending modulus, and length of bending is assumed to be the mesh size, ζ , of the network as calculated by permeability experiments (9).

The stretching displacement, $\delta_{stretch}$, caused by a force pulling on the end of a beam is given by:

$$\delta_{stretch} = \frac{L_{stretch} F_{plt}}{\mu} \quad (\text{S10})$$

where $L_{stretch}$ (80 nm) and μ is the stretch modulus (5×10^{-9} N) as calculated in the previous section above. Using equations S9 and S10, we are able to estimate the displacement imparted upon a fibrin fiber by a platelet assuming a platelet contractile force of 4 nN on a substrate with elasticity of 10 kPa (14). An assumption in this calculation is that the bending and stretching moduli hold over the range of strains predicted.

SUPPORTING FIGURES

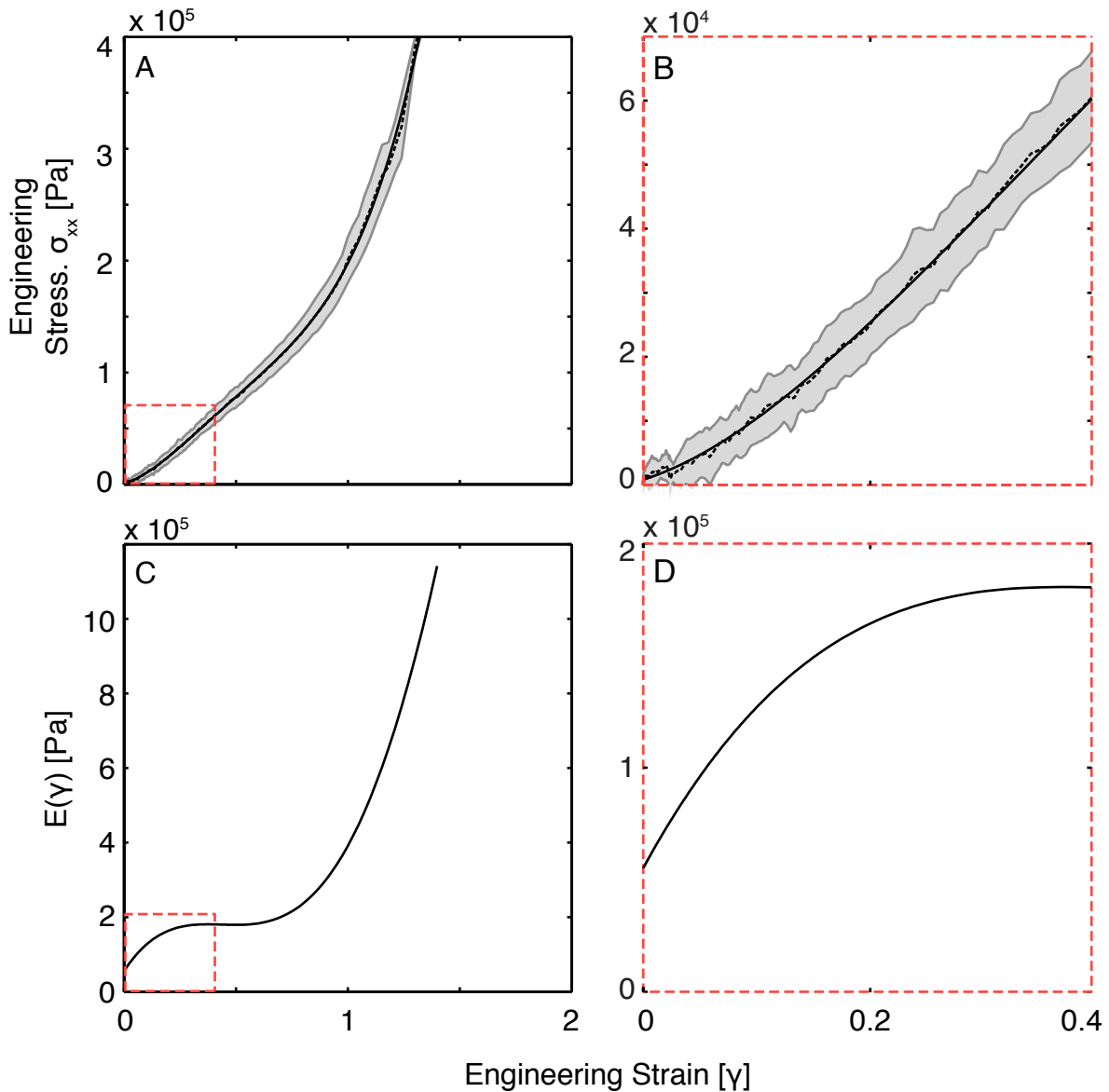


Figure S1. Measurement of engineering stress and calculation of $E(\gamma)$ of a 100 mg/ml fibrin gel formed with 10 nM thrombin. (A) The biaxial stress-strain data with the moving average (---), and 5th degree polynomial fit (—). The shaded region represents the standard deviation ($n=5$). (B) Bi-axial stress-strain data zoomed in to show the fit at low strain. (C) $E(\gamma)$ calculated as the first derivative of the 5th degree polynomial fit. (D) $E(\gamma)$ zoomed in to better show the modulus at low strain.

Supporting Material

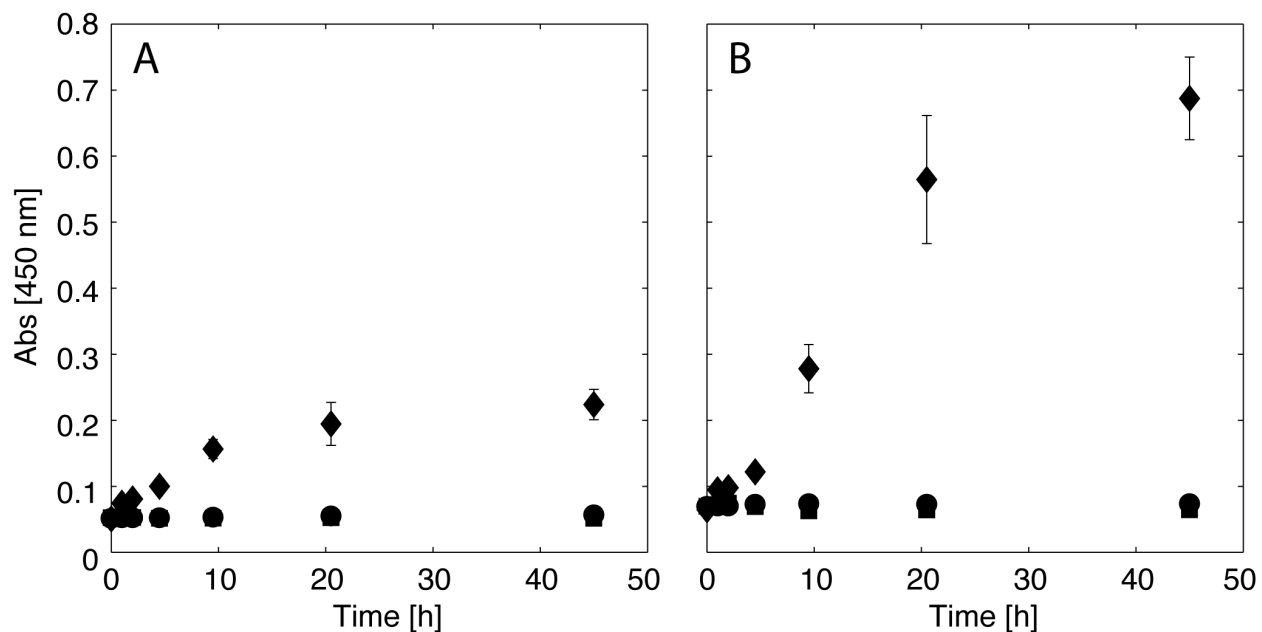


Figure S2. Absorbance of fibrinogen at 450 nm as function of time of (A) Stock fibrinogen solution (12.9 mg/mL) from the supplier and (B) concentrated fibrinogen at 130 mg/ml for solutions incubated at 4 (u), 20 (n), and 37 °C (●). Increases in absorbance are indication of precipitation, which was evident at 4 °C, but no change was observed at 20 and 37 °C

Supporting Material

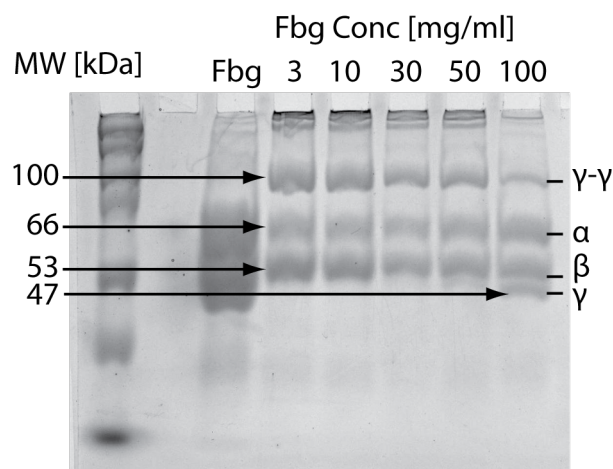


Figure S3. Reducing SDS-PAGE analysis of fibrin gels cross-linking. *Lane 1:* molecular markers, *lane 2:* fibrinogen, *lane 3:* fibrin 3 mg/ml, *lane 4:* fibrin 10 mg/ml, *lane 5:* fibrinogen 30 mg/ml, *lane 6:* fibrinogen 50 mg/ml, *lane 7:* fibrinogen 100 mg/ml. Bands at 66, 53, and 47 kDa corresponding to the α , β , and γ chains of the fibrinogen monomer. The band at 100 kDa corresponding to the γ - γ dimer. All fibrin gels (3 – 100 mg/ml) showed the bands at 100 kDa corresponding to the γ - γ dimer indicating that all gels underwent γ -chain crosslinking. Gels formed with 3 – 50 mg/ml showed the absence of the 47 kDa (γ) band indicating that these gels were completely γ -chain crosslinked. Both the 100 kDa (γ - γ dimer) and the 47 kDa (γ -chain) were present for the 100 mg/ml gel indicating that this gel was crosslinked, but the extent of crosslinking is unknown. All gels showed bands at the very top of the well corresponding to α_n polymer segments. The presence of bands at 66 kDa (α) in all gels show that α -chain crosslinking is incomplete in all gels.

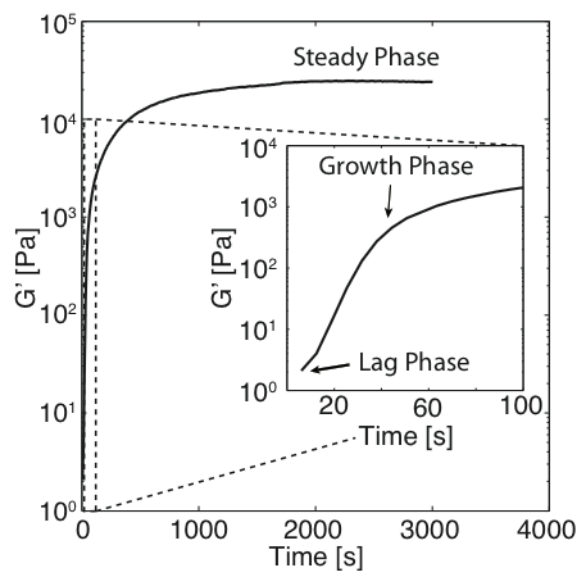


Figure S4. Representative G' as a function time for a 100 mg/ml fibrin gel formed with 100 nM thrombin showing the lag, growth, and steady phases.

SUPPORTING TABLES

Table S1. Dynamic shear storage (G') and loss (G'') moduli of fibrin gels at small strains. Data is presented as the mean and standard deviation (SD) of $n=3$.

Thrombin [nM]	Fibrinogen [mg/mL]	G' at 1 Hz [Pa] (SD)	G'' at 1 Hz [Pa] (SD)
10	3	158 (60)	5.6 (2.8)
10	10	964 (380)	75 (15)
10	30	8200 (1000)	4800 (130)
10	50	12,800 (5300)	700 (51)
10	100	16,500 (7700)	784 (173)
100	3	110 (16)	4.7 (0.6)
100	10	840 (65)	56 (3.0)
100	30	8200 (420)	320 (30)
100	50	19,100 (3100)	800 (100)
100	100	26,200 (3900)	1700 (367)

Supporting Material

Table S2. Rheological measurements of fibrin gels in extensional strain.

Thrombin [nM]	Fibrinogen [mg/mL]	$E(\gamma)$ at γ $= 0$ [Pa] $\times 10^4$	$E(\gamma)$ at γ $= 0.25$ [Pa] $\times 10^4$	Max $E(\gamma)$ [Pa] $\times 10^4$	Modulus Ratio	Stress at break [Pa] \times 10^4 (SD)	Strain at break (SD)
10	10	0.9	3.4	23	6.7	5.1 (4.0)	1.0 (0.39)
10	30	6.3	8.9	20	2.3	19 (4.3)	1.4 (0.17)
10	50	5.8	13.7	60	4.4	33 (10)	1.4 (0.22)
10	100	5.5	16.4	110	6.9	36 (8.2)	1.3 (0.09)
100	10	2.1	3.0	15	5.0	3.9 (1.4)	1.0 (0.09)
100	30	6.0	10.9	39	3.6	25 (6.3)	1.4 (0.18)
100	50	8.3	11.5	66	5.7	27 (10)	1.4 (0.21)
100	100	12.7	20.1	120	5.9	39 (6.8)	1.2 (0.07)

Supporting Material

Table S3. Critical lengths (L_c) and filament length:critical length ratio (L_c/λ_{NA}) for fibrin gels formed at 3 – 100 mg/ml fibrinogen with 10 nM and 100 nM thrombin.

Thrombin [nM]	Fibrinogen [mg/mL]	λ_{NA} [nm]	L_c/λ_{NA}
10	3	4000	0.5
10	10	730	2.7
10	30	83	24
10	50	18	110
10	100	11	190
100	3	4200	0.5
100	10	380	5.2
100	30	140	14
100	50	18	110
100	100	21	96

Supporting References

1. Smith, E.L., B. Cardinali, L. Ping, R. Ariëns, and H. Philippou. 2013. Elimination of coagulation factor XIII from fibrinogen preparations. *Journal of Thrombosis and Haemostasis*. 11: 993–995.
2. Marder, V.J., N.R. Shulman, and W.R. Carroll. 1969. High molecular weight derivatives of human fibrinogen produced by plasmin. I. Physicochemical and immunological characterization. *J. Biol. Chem.* 244: 2111–2119.
3. Larsson, U. 1988. Polymerization and gelation of fibronogen in D₂O. *European Journal of Biochemistry*. 174: 139–144.
4. Laemmli, U.K. 1970. Cleavage of structural proteins during the assembly of the head of bacteriophage T4. *Nature*. 227: 680–685.
5. Bathe, M., C. Heussinger, M.M.A.E. Claessens, A.R. Bausch, and E. Frey. 2008. Cytoskeletal Bundle Mechanics. *Biophysical Journal*. 94: 2955–2964.
6. Collet, J.-P., H. Shuman, R.E. Ledger, S. Lee, and J.W. Weisel. 2005. The elasticity of an individual fibrin fiber in a clot. *Proc Natl Acad Sci U S A*. 102: 9133–9137.
7. Weigandt, K.M., D.C. Pozzo, and L. Porcar. 2009. Structure of high density fibrin networks probed with neutron scattering and rheology. *Soft Matter*. 5: 4321.
8. Shulman, S. 1953. The Size and Shape of Bovine Fibrinogen. *Studies of Sedimentation, Diffusion and Viscosity*. *J. Am. Chem. Soc.* 75: 5846–5852.
9. Wufsus, A.R., N.E. Macera, and K.B. Neeves. 2013. The hydraulic permeability of blood clots as a function of fibrin and platelet density. *Biophysical Journal*. 104: 1812–1823.
10. Storm, C., J.J. Pastore, F.C. MacKintosh, T.C. Lubensky, and P.A. Janmey. 2005. Nonlinear elasticity in biological gels. *Nature*. 435: 191–194.
11. Broedersz, C.P., M. Sheinman, and F.C. MacKintosh. 2012. Filament-Length-Controlled Elasticity in 3D Fiber Networks. *Phys. Rev. Lett.* 108: 078102.
12. Averett, R.D., B. Menn, E.H. Lee, C.C. Helms, T. Barker, and M. Guthold. 2012. A modular fibrinogen model that captures the stress-strain behavior of fibrin fibers. *Biophysical Journal*. 103: 1537–1544.
13. Piechocka, I.K., R.G. Bacabac, M. Potters, F.C. MacKintosh, and G.H. Koenderink. 2010. Structural hierarchy governs fibrin gel mechanics. *Biophysical Journal*. 98: 2281–2289.
14. Lam, W.A., O. Chaudhuri, A. Crow, K.D. Webster, T.-D. Li, A. Kita, J. Huang, and D.A. Fletcher. 2010. Mechanics and contraction dynamics of single platelets and implications for clot stiffening. *Nature Materials*. 10: 61–66.